

# ESTIMATION OF RESERVOIR SEDIMENTATION USING PER-PIXEL AND SUB-PIXEL CLASSIFICATION APPROACHES

S.Saravanan<sup>1</sup>, V.S.Jeyakanthan<sup>2</sup>

<sup>1</sup>Department of Civil Engineering, National Institute of Technology, Tiruchirapalli, India.

<sup>2</sup>Deltaic Regional Centre, National Institute of Hydrology, Kakinada, Andhra Pradesh, India – jeyakanthan05@gmail.com

## Abstract

For the quantification of sediments deposited in the reservoir, the only thematic information that has to be extracted from the satellite data is water spread area at different water levels of the reservoir. Mostly per-pixel methodology such as MLC, minimum distance, band threshold technique are used to classify the water-spread area from the satellite data. One of the limitations of the per-pixel approach in classifying water spread area is that the border pixels that are mixed in nature, representing soil, vegetation class with moisture are also classified as water pixels, thereby giving inaccurate estimate of the water-spread area. To accurately compute the water-spread area, sub-pixel classification or linear mixture model (LMM) approach has been chosen for classifying the water-spread areas of Singoor reservoir, Telangana, South India. LANDSAT8 (OLI) satellite data pertaining to the year 2014 were used to extract the water-spread area of the reservoir by band threshold and sub-pixel classification approaches. It was ascertained that the estimated capacity of the reservoir from band threshold and sub-pixel approaches were 695.71 Mm<sup>3</sup> and 690.53 Mm<sup>3</sup> respectively. The difference in capacity between the period 1987 (hydrographic survey) and 2014 (per-pixel and sub-pixel approaches) reveals the amount of sedimentation deposited in the reservoir. If uniform rate of sedimentation is assumed from 1987 to 2014, it is ascertained that the annual rate of sedimentation in Singoor reservoir using per-pixel and sub-pixel approaches are 2.70 Mm<sup>3</sup> and 2.71 Mm<sup>3</sup> respectively.

**Keywords:** water-spread area, trapezoidal formula, reservoir capacity, hydro-graphic survey, fraction images

-----\*\*\*-----

## INTRODUCTION

Natural processes, such as erosion in the catchment area, movement of sediment and its deposition in various parts of the reservoir, require careful consideration in the planning of major reservoir projects. The silt that is deposited at different levels reduces the storage capacity of the reservoir (Smith and Pavelsky 2009). Reduction in the storage capacity beyond a limit prevents the reservoir from fulfilling the purpose for which it is designed. Periodic capacity surveys of the reservoir help to assess the rate of sedimentation and reduction in storage capacity. Conventional techniques for the estimation of the capacity of a reservoir, such as hydrographic survey and inflow-outflow approaches, are cumbersome, time consuming and expensive, and they involve significant manpower. As an alternative to conventional methods, the remote sensing technique provides cost- and time-effective estimation of the live capacity of a reservoir (Sabastian 1995). Multi-date satellite remote sensing data provide information on elevation contours, in the form of water spread area, at different water levels of a reservoir. The water spread area thus interpreted from the satellite data is used as an input into a simple volume estimation formula to calculate the capacity of a reservoir. Such work has been reported by Jeyakanthan (2002) for the Poondi Reservoir in India, Goel (2002) for the Bargi Reservoir in India, Jain (2002) for the Bhakra Reservoir in India and Peng (2006) for the Fegman Reservoir in China.

To quantify the capacity of a reservoir, the only thematic information that has to be extracted from the satellite data is the water spread area at different water levels of the reservoir (Morris and Fan 1998, Peng 2006). Different approaches to delineate various thematic information from the remote sensing digital data, such as maximum likelihood classification, minimum distance to mean classification and the band threshold method, adopt the per-pixel based methodology and assign a pixel to a single land cover type (Jensen 1996, Bastin 1997); whereas in reality, a single pixel may contain more than one type of land cover (known as a mixed pixel). Mixed pixels are common especially near the boundaries of two or more discrete classes (Foody and Cox 1994, Ibrahim et al. 2005). The boundary pixels of the water spread area that are mixed in nature, representing soil or vegetation with moisture, are classified as water pixels when a per-pixel based approach is applied, thereby producing an inaccurate estimate of the water spread area. To accurately compute the water spread area to the maximum possible extent, thereby reducing the error in the estimation of the capacity of a reservoir, a sub-pixel or linear mixture model (LMM) approach has been chosen for classifying the boundary pixels of the water spread area from different water levels of the Singoor Reservoir located in the Telangana state of India.

## 1. STUDY RESERVOIR

The Singoor Reservoir is a major irrigation project built across the river Manjira, which is one of the tributaries of the Godavari River, the second largest river in the Indian subcontinent. The project is located near Singoor village, Medak District, which is at a distance of 100 km from Hyderabad, the capital city of Telangana state. The total length of the dam is 7.52 km, which includes a 327 m long overflow masonry dam in the river gorge portion and an 81 m non-overflow masonry dam flanked on both sides by earthen embankments. The climate of the sub-basin is characterised by a hot summer and a mild winter. The monsoon season begins early in the month of June and continues up to the end of October. The principal type of soil present in the catchment area, apart from the red soil, is black cotton mixed soil. Due to various activities in the catchment area, the black cotton soil is easily eroded and an enormous amount of silt is carried into the stream that drains into the Manjira River. The eroded soil eventually get deposited into the Singoor Reservoir and drastically reduces its capacity. Hence, estimation of the capacity is a problem when studying this reservoir.

### 2.1 Satellite Data Used

The image data used in this study were acquired by LANDSAT8-OLI satellite which provides a spatial resolution of 30 m in eleven different spectral bands. L8 level 1 product has been used in this study. The different dates of the satellite data used and the respective water level during the pass of the satellite over the reservoir are given in Table 1. Reservoir water level data and the hydrographic survey details have been collected from the Singoor Reservoir authority responsible for the maintenance and operation of the reservoir.

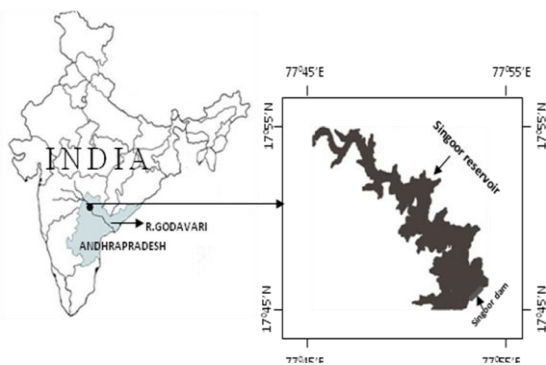


Figure 1. Location map of the Singoor

Sl.No.	Date of Pass	Water Level (m)
1.	10.01.2014	523.01
2.	15.03.2014	522.27
3.	16.04.2014	520.79
4.	18.05.2014	520.25
5.	09.10.2014	519.47

Table.1 Date of satellite images used and their water levels.

## 2. METHODOLOGY

The changes in the water spread could be accurately estimated by analysing the areal spread of the reservoir at different elevations over a period of time using the satellite image data (Morris and Fan 1998, Smith and Pavelsky 2009). Per-pixel and sub-pixel approaches have been used in this study to extract the water spread area of the reservoir. Estimated water spread areas were used in a simple volume estimation formula to compute the storage capacity of the reservoir. Estimation of the water spread area and the computation of the capacity of the reservoir are discussed in the following sections.

### 2.1 Per-Pixel Based Approach

Water reflects most of the visible wavelengths, but the energy at the near-infrared (NIR) wavelength is almost absorbed by the water, thus providing a significant contrast between land and water in the NIR images (Lillesand and Kiefer 2004). This contrast helps in extracting the water spread area of the reservoir. Different procedures have been adopted by many researchers (Chopra et al. 2001, Dechka et al. 2002, Jain et al. 2002, Rathore 2006, Alsdorf 2007) for water body identification in wetland areas and reservoirs, each adopting the per-pixel based approach. Among these procedures, the band threshold approach is a relatively easy and valid method for identifying the water body. It has also been suggested that this per-pixel based approach can give acceptable estimates of the area of the water body if the NIR band is used (Goel 1996, Jain 2002). Therefore, in the per-pixel based approach, the band threshold technique was adopted to extract the water pixels that correspond to various water levels of the reservoir. The following model equation has been used in the image processing software to delineate the water spread area of the reservoir. The adopted algorithm states that:

$$\text{if } P_{V-NIR} > T_{L-NIR} \text{ and } P_{V-NIR} < T_{H-NIR} \text{ then} \quad (1)$$

the pixel is in the water spread area, where  $P_{V-NIR}$  is the pixel value in NIR band and  $T_{L-NIR}$  and  $T_{H-NIR}$  are the lower and higher thresholds for the NIR band.

Because the absorption of electromagnetic radiation by water is at a maximum in the NIR spectral region, the digital number (DN) of water pixels is considerably lower than that corresponding to other land cover types. Even if the water depth is shallow, the increased absorption in the NIR band will restrict the DN value to less than that of the green and red bands. If the soil is exposed (possibly saturated) at the surface, the reflectance will be as per the signature of the soil, which increases with wavelength in this spectral range. Thus, by following this algorithm (Equation 1) water pixels that belong to a particular water level of the reservoir were extracted. The NIR band (Band5) of LANDSAT8 which have band width from 0.851 to 0.879  $\mu\text{m}$  has been used in this study to extract the water spread-area from all the five images.

### 2.2 Sub-Pixel Based Approach

The sub-pixel classifier uses the linear unmixing technique that allows for the identification of the "material of interest"

and the determination of its “material part fraction” or cover percentage within a pixel.

Linear spectral unmixing is a perfect approximation for calculating the abundance or fraction of an end-member in an image pixel. The LMM classification technique attempts to estimate the proportions of specific classes that occur within each pixel using the linear mixing approach (Foody 1996, Min Xu 2005). In this study, the border pixels of reservoir water spread area which are the main sources of mixed pixels were estimated using the linear spectral unmixing approach.

The basic assumption of the LMM is that the measured reflectance of a pixel is the linear sum of the reflectance of the components that make up the pixel. The basic hypothesis is that the image spectra are the result of mixtures of surface materials, shade and clouds and that each of these components is linearly independent from the others (Bosdogianni et al. 1997, Atkinson 1997). Linear unmixing also assumes that all of the materials within the image have sufficient spectral contrast to allow their separation. In a soft classification, the estimated variables (the fractions or proportions of each land cover class) are continuous, ranging from 0 to 100 percent coverage within a pixel. Settle and Drake (1993) and Foody and Cox (1994) proposed a mathematical expression for linear spectral unmixing. The theory behind this is that a series of end-members present within a pixel contribute to the overall spectral signature of that pixel. Hence, the spectral signature of a pixel would be derived from the sum of the products of the single spectrum of each end-member it contains, each weighted by a fraction, plus a residue as explained by the following mathematical model:

$$R_i = \sum_k f_k R_{ik} + E_i \quad (2)$$

$$\text{where } \sum_k f_k = 1 \quad (3)$$

$$\text{and } 0 \leq f_k \leq 1 \quad (4)$$

$i = 1, \dots, m$  (number of spectral bands)

$k = 1, \dots, n$  (number of end-members)

$R_i$  = Spectral reflectance of band  $i$  of a pixel which contains one or more end-members

$f_k$  = Proportion of end-member  $k$  within the pixel

$R_{ik}$  = Known spectral reflectance of end-member  $k$  within the pixel in band  $i$

$E_i$  = Error for band  $i$  (Difference between the observed pixel reflectance  $R_i$  and the reflectance of that pixel computed from the model).

Equations 2 and 3 introduce the constraints that the sums of the fractions are equal to one and they are non-negative. To solve for  $f_k$ , the following conditions must be satisfied: (i) selected end-members should be independent of each other, (ii) the number of end-members should be less than or equal to the spectral bands used, and (iii) selected spectral bands should not be highly correlated.

In this study, linear spectral unmixing is adopted based on the equations described below to segregate the actual information within a pixel of an image:

$$\begin{aligned} R1 &= F_{\text{water}} * R1_{\text{water}} + F_{\text{veg}} * R1_{\text{veg}} + F_{\text{soil}} * R1_{\text{soil}} + \epsilon1 \\ R2 &= F_{\text{water}} * R2_{\text{water}} + F_{\text{veg}} * R2_{\text{veg}} + F_{\text{soil}} * R2_{\text{soil}} + \epsilon2 \\ R3 &= F_{\text{water}} * R3_{\text{water}} + F_{\text{veg}} * R3_{\text{veg}} + F_{\text{soil}} * R3_{\text{soil}} + \epsilon3 \end{aligned} \quad (5)$$

where,

$R1$ ,  $R2$  and  $R3$  represent the signal recorded by the satellite (DN values) in the green, red and NIR bands of the LISS-III sensor.

$F_{\text{water}}$ ,  $F_{\text{veg}}$  and  $F_{\text{soil}}$  are the fraction of the pixel covered by water, vegetation and soil.

$R1_{\text{water}}$ ,  $R2_{\text{water}}$  and  $R3_{\text{water}}$  represent the DN of water in each of the three spectral bands (water end-members).

$R1_{\text{veg}}$ ,  $R2_{\text{veg}}$  and  $R3_{\text{veg}}$  represent the DN of vegetation in each of the three spectral bands (vegetation end-members).

$R1_{\text{soil}}$ ,  $R2_{\text{soil}}$  and  $R3_{\text{soil}}$  represent the DN of soil in each of the three spectral Bands (soil end-members).

$\epsilon1$ ,  $\epsilon2$  and  $\epsilon3$  are the error components of band 1, 2 and 3.

The system of linear equations shown above can be solved by a least squares solution that minimizes the sum of squares of errors. To maintain the consistency between the per-pixel and sub-pixel processes DN values were used as input parameter in the equation 1 & 5.

The sub-pixel based approach was applied to determine the proportion or fraction of the water class that exists in the peripheral pixels of the reservoir. The first step executed in the sub-pixel approach was the selection of the pure pixels (known as end-members) belonging to a specific class. In general, the border pixels may contain any combination and proportion of water, vegetation and soil classes. Hence, these three classes were chosen to represent the end-members. The scatter plot method was used to identify the end-members. The locations of the end-members in the image data were identified from the extremes of the scatter plot. The identified end-member spectra were supplied as input to the LMM approach. The output of the model run contains three images labelled as water-, soil- and vegetation- fraction images. A description of the fraction images is given in section 4.2.

### 3.3 Computation Of Volume Between Successive Water Levels

Traditionally the reservoir volume between two consecutive reservoir water levels was computed using the prismoidal formula, the Simpson formula or the trapezoidal formula (Patra 2001). Of these, the trapezoidal formula has been most widely used for the computation of volume (Goel and Jain 1996, Morris and Fan 1998, Rathore 2006) in Indian reservoirs. The water spread area estimated using the per-pixel and sub-pixel approaches were separately used as an input to the volume estimation formula to determine the volume at different water segments of the reservoir. In this study the volume between two consecutive reservoir water levels was computed using the following trapezoidal formula:

$$V = H * (A1 + A2 + \sqrt{A1 * A2}) / 3 \quad (6)$$

where  $V$  is the volume between two consecutive water levels,  $A_1$  and  $A_2$  are the water spread areas at the reservoir water levels 1 and 2 respectively and  $H$  is the difference between these two water levels.

### 3.4 Computation Of Storage Capacity Of The Reservoir

The volumes computed (using equation 6) between different water levels (i.e., from minimum draw down level (MDDL) to full reservoir level (FRL)) were added together to calculate the cumulative or storage capacity of the reservoir.

### 3.5 Estimation Of Reservoir Sedimentation

The difference in storage capacity between any two periods produces the amount of sedimentation deposited in the reservoir. The annual rate of sedimentation could be arrived by dividing the total amount of sediment deposited during that period.

## 4. RESULTS AND DISCUSSION

### 4.1 Computation Of Reservoir Capacity By The Per-Pixel Approach

Five different water levels varying from 519.47 m to 523.01 m of the reservoir were selected for the year 2014 based on the availability of cloud free satellite data to estimate the water spread of the reservoir. To extract the water pixels from the images using the per-pixel approach, the algorithm presented in Equation 1 was used. This algorithm requires minimum and maximum threshold DNs from the NIR band of the five satellite images used in the study. With the help of the algorithm, the pixels which contain a DN between the given minimum and maximum threshold values were labelled as water pixels. Basic statistical parameters of an image that could be obtained using the image processing software were utilised to determine the minimum pixel values of the water spread area. Landsat8 data is supplied with 16 bit unsigned integer format. Hence the grey level varies from 0 to 65536. The minimum DN values of the water spread area are 6048, 5892, 7137, 7292 and 7081 for the images pertaining to the months January, March, April, May and October respectively.

The periphery of the reservoir contains low water depth and due to the presence of mixed pixels they exhibit maximum DN values. The maximum DN values used to extract the water spread area are 6945, 7250, 10150, 11300 and 12200 pertaining to the images in the chronological order. The locations of these pixels in the water spread area were also verified, and showed that the pixels with low DN were located in the deeper and central portion of the water spread area of the reservoir. The analysis of DN values of the water body show that the pixel value increases towards the periphery of the water body and the border pixels contain the maximum DN.

The total number of water pixels that were extracted was multiplied by the area (30 m x 30 m) of a single pixel to

compute the water spread area. The same technique was adopted to convert the extracted pixels into the water spread area in all the five images used in this study.

The water spread area thus estimated in each image using the per-pixel approach has been used as an input to the trapezoidal formula (Equation 6) to calculate the consecutive volumes of the reservoir. The storage capacity between the bed level (500.17 m) of the reservoir and the lowest observed water level (519.47 m) could not be estimated using satellite data due to presence of water column between these levels. Therefore, the capacity (323.93 Mm<sup>3</sup>) between these two levels was adopted from the 2005 capacity survey conducted by this author using remote sensing data. Above the lowest observed level (519.47 m), the estimated capacities between the consecutive water levels were added up to arrive at the cumulative capacity of the reservoir at the maximum observed level (523.01 m). The estimated cumulative capacity of the reservoir at the water level 523.01 m (near FRL) using the per-pixel classification approach was 695.71 Mm<sup>3</sup>.

### 4.2 Computation Of Reservoir Capacity By The Sub-Pixel Approach

The fraction images generated using the sub-pixel approach described in the methodology section contain a wealth of information about the reservoir water-spread area. Each fraction image corresponds to only single type of land cover and hence information pertaining to single land cover can be extracted. For example, the pixels in the water fraction image provide information only on the proportion or amount of water contained in the pixel. Likewise, the vegetation and soil fraction images provide information on the proportions of their respective classes only. However, in this study the interest is only to determine the amount of water present in the border pixels of the reservoir. The value of the pixels in the fraction image ranges from 0 to 1. A pixel from the water fraction image having a value of 0 indicates that there is no water at all in that pixel, whereas a pixel having a value of 0.74 indicates that 74% of the area of the pixel is occupied by water while a pixel value of 1 indicates that 100% of the area of the pixel is occupied by water (i.e., the pixel is fully occupied by water). Therefore, for a pixel having a value of 0.7, the area of water occupied by that pixel is 630 m<sup>2</sup> (0.7 x 30 m x 30 m).

After examining the peripheral pixels it was ascertained that a small number of the border pixels contain water spread area less than 10%. Hence, a threshold value of 10% was selected and used for analysis. The pixels representing the peripheral portion of the reservoir, which have a minimum value of 0.1 in the water fraction image (i.e., a pixel with a minimum of 10% of its area containing water) were isolated from the water-fraction image and the area covered by water in these peripheral/border pixels was estimated. The number of pixels that contain 100% water was also determined. By summing the area occupied by these two types of pixels, the total water spread area corresponding to a particular water level of the reservoir was computed. This exercise was carried out for all the five images used in the study. The water spread area thus estimated was again used as an input to the trapezoidal

formula to compute the storage capacity or cumulative capacity of the Singoor Reservoir using the sub-pixel classification approach.

It is worth mentioning that a pixel containing 65% water may be labelled as containing 100% water by the per-pixel approach. Thus, the water spread area is overestimated. Conversely, if the pixel contains 40% water, then the entire pixel is not considered for the water spread area estimation. Hence, the water spread area is underestimated. Such errors due to overestimation or underestimation do not occur in the sub-pixel approach. Thus, the sub-pixel approach reduces the error imposed by the per-pixel approach. The estimated cumulative capacity of the reservoir at the water level of 523.01 m (near FRL) using the sub-pixel approach was 690.53 Mm<sup>3</sup>.

### 4.3 Computation Of Reservoir Sedimentation

The difference in capacity between the period 1987 (impoundment survey of the reservoir) and the present capacity (2014) reveals the amount of sedimentation deposited in the reservoir. During 1987 the capacity of Singoor reservoir was 763.61 Mm<sup>3</sup> at the water level 523.01 m. If uniform rate of sedimentation is assumed for a period of 27 years from 1987 to 2014, it is ascertained that the annual rate of sedimentation in Singoor reservoir using per-pixel and sub-pixel approaches are 2.70 Mm<sup>3</sup> and 2.71 Mm<sup>3</sup> respectively.

## 5. CONCLUSIONS

High spatial-resolution image data enables accurate mapping of terrain features. The use of high spatial resolution satellite image data, however, is constrained by factors such as cost and the smaller area covered by the sensor. Hence, in hydrological applications estimating the water spread area using high resolution data may be difficult because a reservoir may not be imaged in a single pass of the satellite and atmospheric conditions would be different from path to path (Hung and Wu 2005). An alternative method to overcome such constraints is the use of the sub-pixel based approach. The simplest methodology for such an approach is the linear mixture model, which has been demonstrated in this study to accurately estimate the capacity and in turn the annual rate of sedimentation of the Singoor Reservoir in India.

The capacity and rate of sedimentation is better estimated if the remote sensing survey is carried out for the full reservoir level i.e from the minimum draw down level (MDDL) to full reservoir level. In this study the satellite data could not be utilized up to MDDL due to the presence of water column above MDDL. Estimation of capacity using hydrographic survey was carried out for defined water level intervals whereas the satellite data could not be obtained for the same water levels. This mismatch in water levels between the hydrographic survey and satellite data may impose some amount of inaccuracy in estimating the rate of sedimentation of the reservoir.

## ACKNOWLEDGEMENTS

The author is thankful to the USGS for providing the satellite data. He is also thankful to the Singoor dam officials for providing the required reservoir details.

## REFERENCES

- [1] Alsdorf, D.E., Rodriguez, E., Lettenmaier, D.P. (2007). "Measuring surface water from space." *Reviews of Geophysics*, 45 (2), 1–24.
- [2] Atkinson, P.M. (1997). "Mapping sub-pixel proportional land cover with AVHRR imagery." *International Journal of Remote Sensing*, 18 (4), 917-935.
- [3] Bastin, L. (1997). "Comparison of fuzzy c-means classification, linear mixture modelling and MLC probabilities as tools for unmixing coarse pixels." *International Journal of Remote Sensing*, 18 (17), 3629-3648.
- [4] Bosdogianni, P., Petrou, M., and Kittler, J. (1997). "Mixed pixel classification with robust statistics." *IEEE Transactions on Geoscience and Remote Sensing*, 35 (3), 551-559.
- [5] Chopra, R., Verma, V.K. and Sharma, P.K. (2001). "Mapping, monitoring and conservation of Harike wetland ecosystem, Punjab, India through remote sensing." *International Journal of Remote Sensing*, 22 (1), 89-98.
- [6] Dechka, J.A., Franklin, S.E., Watmough, M.D., Bennett, R.P. and Ingstrup, D.W. (2002). "Classification of wetland habitat and vegetation communities using multitemporal IKONOS imagery in southern Saskatchewan." *Canadian Journal of Remote Sensing*, 28 (5), 679–685.
- [7] Foody, G. M., and Cox, D. P. (1994). "Sub-pixel land cover composition estimation using a linear mixture model and fuzzy membership functions." *International Journal of Remote Sensing*, 15 (3), 619-631.
- [8] Foody, G.M. (1996). "Approaches for the production and evaluation of fuzzy land cover classifications from remotely sensed data." *International Journal of Remote Sensing*, 17 (7), 1317-1340.
- [9] "Goel, M. K., and Jain, S. K., 1996. Evaluation of reservoir sedimentation using multi-temporal IRS-1A LISS II data." *Asian Pacific Remote Sensing & GIS Journal*, 8 (2), 39-43.
- [10] Goel, M.K., Jain, S.K., and Agarwal, P.K., (2002). "Assessment of sediment deposition rate in Bargi Reservoir using digital image processing." *Hydrological Sciences Journal*, 47(S), S81-S92.

- [11] Hung, M.C., and Wu, Y.H. (2005). "Mapping and visualizing the Great Salt Lake landscape dynamics using multi-temporal satellite images-1972-1996." *International Journal of Remote Sensing*, 26 (9), 1815-1834.
- [12] Ibrahim, M. A., Arora, M. K., and Ghosh, S. K., (2005). "Estimating and Accommodating uncertainties through soft classification of remote sensing data." *International Journal of Remote Sensing*, 26 (14), 2995-3007.
- [13] Jain, S.K., Singh, P., and Seth, S.M. (2002). "Assessment of sedimentation in Bhakra Reservoir in the western Himalayan region using remotely sensed data." *Hydrological Sciences Journal*, 47 (2), 203-212.
- [14] Jensen R.J. (1996). "Introductory Digital Image Processing : A remote sensing perspective". 2nd edition, (London: Prentice Hall International Ltd.,).
- [15] Jeyakanthan, V.S., Sreenivasulu, V., Rao, Y.R.S., Ramasastri, K.S., (2002). "Reservoir capacity estimation using satellite data. IAPRS & SIS." Vol.34, Resources and Environmental Monitoring, Hyderabad, India, 863-866.
- [16] Lillesand, T.M. and Kiefer, R.W. (1994). "Remote Sensing and Image Interpretation." 3rd edition, (New York: John Wiley & Sons).
- [17] Min Xu, Watanachaturaporn, P., Varshney, P. K., and Arora, M.K. (2005). 'Decision Tree Regression for Soft Classification of Remote Sensing Data.'" *Remote Sensing of Environment*, 97 (3), 322-336.
- [18] Morris, G.L., and Fan Jiahua. (1998). "Reservoir Sedimentation Handbook." (New York: McGraw-Hill Book Co).
- [19] Patra, K.C. (2001). "Hydrology and Water Resources Engineering." (New Delhi: Narosa Publishing House).
- [20] Peng Dingzhi, Shenglian Guo., Pan Liu, Ting Liu., (2006). "Reservoir storage curve estimation based on remote sensing data." *Journal of Hydrologic Engineering*, 11, 165-172.
- [21] Rathore, D.S., Anju Choudhary, and Agarwal, P.K. (2006). "Assessment of sedimentation in Harakud Reservoir using digital remote sensing technique." *Journal of the Indian Society of Remote Sensing*, 34, 344-383.
- [22] Sabastin, M., Rao, P.P.N., Jayaraman. V., and Chandrasekhar, M.G.(1995). "Reservoir storage loss assessment and sedimentation modeling through remote sensing techniques." *Proceedings of 6th Inter. Symp. River sedimentation on Management of Sediment – Philosophy, Aims and Techniques*, New Delhi, India.
- [23] Settle, J.J., and Drake, N.A. (1993). "Linear mixing and the estimation of ground cover proportions." *International Journal of Remote Sensing*, 14 (6), 1159-1177.
- [24] Smith, L.C., and Pavelsky, T.M. (2009). "Remote sensing of volumetric storage changes in lakes." *Earth Surface Process and Landforms*, 34, 1353 – 1358.